

Demulsification Efficiency of Some Novel Styrene/Maleic Anhydride Ester Copolymers

A. M. Al-Sabagh,¹ M. R. Noor El-Din,¹ R. E. Morsi,² M. Z. Elsabee²

¹Department of Petroleum Applications, Egyptian Petroleum Research Institute, 1 Ahmed El-Zomor Street, Nasr City, 11727, Cairo, Egypt

²Department of Chemistry, Faculty of Science, Cairo University, Cairo, Egypt

Received 3 February 2007; accepted 3 June 2007

DOI 10.1002/app.27124

Published online 12 February 2008 in Wiley InterScience (www.interscience.wiley.com).

ABSTRACT: Four demulsifiers were prepared in three steps. In the first step, styrene and maleic anhydride were copolymerized. In the second step, a long-chain alcohol (dodecanol) was reacted with the prepared copolymer to form the monoesterified copolymer. In the final step, the resulting product was further esterified with poly(propylene oxide) (PPO)–poly(ethylene oxide) (PEO) block copolymers of different molecular weights (1.1, 2.5, 3.0, 5.0, and 8.0×10^3) and different PPO/PEO ratios. The demulsification efficiency of these demulsifiers was investigated with the bottle test (Sany glass). The effects of the molecular weight and ratio of the PPO–PEO block copolymers on the demulsification efficiency were studied. The demulsifica-

tion efficiency could be enhanced from 66% by an individual demulsifier to 100% by demulsifier blends. The surface-active and thermodynamic properties of the prepared demulsifiers were measured at 25, 35, and 45°C. The kinetics of the demulsification process were photographed with a binocular microscope. The demulsification mechanism was found to occur in three stages, that is, adsorption and flocculation, coalescence, and channel formation followed by separation. © 2008 Wiley Periodicals, Inc. *J Appl Polym Sci* 108: 2301–2311, 2008

Key words: block copolymers; functionalization of polymers; hydrophilic polymers; surfactants

INTRODUCTION

Crude oil commonly exists in the form of water-in-oil (W/O) emulsions. These emulsions are formed during the production of crude oil, which is often accompanied by water. Natural surfactants such as asphaltenes, resins, and carboxylic acids and solids such as clay and waxes stabilize these emulsions. The emulsions have stability ranging from a few minutes to years, depending on the nature of the crude oil and the extent of water. It is essential to break these emulsions before transportation through pipelines and before refining.^{1,2} Chemical demulsification is an important method of treating W/O emulsions. Thousands of surfactants have been synthesized; a literature survey turns up 2000–3000 patents referring directly to this subject.³ Commercial demulsifiers are polymeric surfactants such as copolymers of poly(ethylene oxide) (PEO) and poly(propylene oxide) (PPO) or alkyl phenol/formaldehyde resins or blends of different surface-active substances. These demulsifiers are surface-active agents and develop a high surface area at the crude water/oil interfaces. This results in the replacement of rigid films of natural crude oil sur-

factants by a film that is conducive to coalescence of water droplets.

The efficiency with which a surfactant acts as a demulsifier depends on many factors. Such factors include the distribution of the demulsifier throughout the bulk volume of the emulsion, the partitioning of the demulsifier between the phases, the temperature, the pH, and the salt content of the aqueous phase. Other factors of importance are the mode of injection of the demulsifier, its concentration, the type of carrier solvent, the amount of water in the emulsion, and the age of the emulsion.^{4,5} The mechanism of demulsification and the principal role of the surfactant in the destabilization of emulsions have been studied by many researchers.^{6–9} The demulsification mechanism of demulsifiers is quite complicated, and no demulsifier can be applied to break all kinds of crude oil emulsions.¹⁰ The demulsification ability of a demulsifier is mainly controlled by two factors: the hydrophilic–hydrophobic ratio and the ability to break the interfacial film.¹¹ The structure of the demulsifier can influence both factors. Shetty et al.¹² concluded that a demulsifier containing a high percentage of hydrophilic groups and having a low molecular weight could perform very well, Marquez-Silva et al.¹³ proposed an empirical model that established a relation between the nature of the crude oil, the associated water salinity, and the demulsifier hydrophilicity. This work concentrates

Correspondence to: M. Z. Elsabee (mzelsabee@yahoo.com).

on two objects: (1) preparing water- and oil-soluble copolymers derived from a styrene/maleic anhydride copolymer (PSMA) and (2) evaluating these polymers as demulsifiers for breaking up water in petroleum oil emulsions.

EXPERIMENTAL

Materials

Maleic anhydride (Merck, Germany) was recrystallized from chloroform. The melting point of the obtained crystals was 54–56°C. Styrene was mixed with a 10% sodium hydroxide solution for 1 h to remove the inhibitors, washed with distilled water, dried on anhydrous sodium sulfate, and then distilled *in vacuo* before use. The initiator, azobisisobutyronitrile (AIBN) (Aldrich, Germany), was recrystallized from methanol. All other chemicals were used as received.

Crude oil

An asphaltenic crude oil was obtained from Petrobel Co. (Egypt). The general physicochemical properties of this crude oil are shown in Table I.

Copolymerization of styrene with maleic anhydride

Into a 500-mL, flat-bottom flask, 0.5 mol of styrene and 0.5 mol of maleic anhydride were dissolved in 200 mL of acetone. The reaction mixture was purged with N₂ gas for about 5 min and then kept at 60°C for 4 h in the presence of the AIBN initiator.¹⁴ The copolymer that formed was precipitated in excess petroleum ether and was purified by reprecipitation from acetone into petroleum ether (60/80). Finally, the precipitated copolymer was dried *in vacuo* until a constant weight was obtained. The product was PSMA. The molecular weight of PSMA was measured viscometrically with the Mark–Houwink equation:

$$[\eta] = kM^\alpha \quad (1)$$

where $[\eta]$ is the intrinsic viscosity, k is 5.07×10^{-5} , and α is 0.81. The molecular weight was found to be 2.66×10^5 .

TABLE I
Physicochemical Properties of the Crude Oil

Specification	Method	Results
Specific gravity at 60/60°F	ASTM D 1298	0.973
API gravity at 60°F	ASTM D 1298	35.29
Kinematic viscosity at 40°C (C. St.)	ASTM D 445	14.97
Asphaltene content (wt %)	IP 143/57	8.5
Pour point (°C)	ASTM D 97	+18
Water content (vol %)	IP 74/70	30
BS&W (vol %)	ASTM D 4007	30.5

C. St, Cent stock; API, American Petroleum Institute; BS&W, basic salt and water contents.

Monoesterification of PSMA

In a 1-L, flat-bottom flask fitted with a Dean–Stark trap and a condenser, 1 mol of PSMA was esterified with 1.2 mol of dodecyl alcohol. The reaction ingredients were refluxed in toluene in the presence of 0.01% *p*-toluene sulfonic acid as a catalyst with continuous stirring until the theoretical amount of water was collected and a homogeneous solution was obtained. Then, the solvent was distilled off *in vacuo*, and the product was precipitated in an excess amount of methanol; then, the product was dried to a constant weight. The oil-soluble product was a dodecanoyl monoester of PSMA (MPSMA).

Mixed diesterification of PSMA

MPSMA and poly(ethylene oxide–propylene oxide) block copolymers of different molecular weights (1.1, 2.5, 3.0, 5.0, and 8.0×10^3) in a 1 : 10 (w/w) ratio were dissolved in toluene and charged into a two-necked flask connected to a Dean–Stark trap and a condenser in the presence of 0.01% *p*-toluene sulfonic acid as a catalyst. The reactants were refluxed at 110°C with continuous stirring until the theoretical amount of water was collected. The product was a mixed diester of MPSMA (DPSMA).

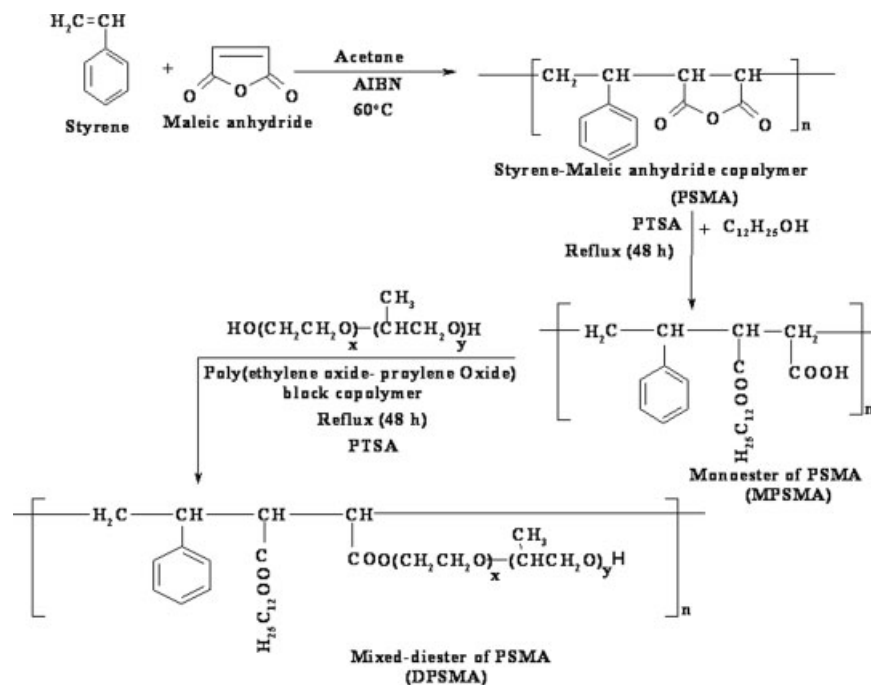
The chemical reaction of PSMA, MPSMA and DPSMA is shown in Scheme 1.

Preparation of water in a crude oil emulsion

In a 250-mL beaker, the crude oil was stirred at 25°C and 2000 rpm while seawater was added gradually to the crude oil until the two phases became completely homogeneous.¹⁵ The emulsions were prepared at different percentage ratios of water to crude oil (30 : 70, 50 : 50, and 70 : 30).

Bottle test

The graduated bottle test (Sany glass) was used to estimate the efficiency of the demulsifiers toward resolving W/O emulsions. Each demulsifier was dissolved in xylene (20% active material) and then added to 100 mL of the previously prepared emulsion at different concentrations (ppm). The mixture was added to a 100-mL Sany glass and then was shaken vigorously for 1 min. The bottle was placed in a thermostated water bath at 60°C. Water separation (mL) was observed at different times depending on the efficiency of the demulsifier under investigation. A blank was considered in each set of experiments.¹⁶



Where: for PPO-PEO block copolymer,

M.wt. = 2500,	$x = 26$ and $y = 24$,	—————>	D1
M.wt. = 3000,	$x = 34$ and $y = 26$,	—————>	D2
M.wt. = 5000,	$x = 68$ and $y = 34$,	—————>	D3
M.wt. = 8000,	$x = 127$ and $y = 41$,	—————>	D4

D: samples used as demulsifiers

Scheme 1 Preparation of PSMA, MPSMA, and DPSMA.

Surface tension measurements

The prepared polymeric water-soluble surfactants were subjected to surface tension measurements. Different molar concentrations of each surfactant were prepared, and their surface tension was determined at different temperatures with a Kruss model K9 apparatus (Germany). About 40 mL of each surfactant, placed in a double-jacket glass cell connected to a thermostated oil bath for maintaining the adjusted temperature, was used for measuring the surface tension at 25, 35, and 45°C. Doubly distilled water was used for preparing the different concentrations of the investigated surfactants. The surface tension of the doubly distilled water was measured at the same temperatures as a reference. The critical micelle concentration (cmc) for the prepared surfactants was determined by the plotting of the surface tension of the surfactant solution against the logarithm of the solute concentration. The cmc values were determined from the abrupt change in the slope of plots of the surface tension versus the logarithm of the solute concentration. It must be mentioned that micelles of surfactants are formed in bulk aqueous

solutions above a given concentration for each surfactant, and this concentration is known as cmc.

Surface tension parameters

Effectiveness of surface tension reduction

The values of the surface tension at cmc (γ_{cmc}) were used to calculate the values of the surface pressure at cmc (π_{cmc} ; effectiveness) with the following equation:^{17,18}

$$\pi_{\text{cmc}} = \gamma_0 - \gamma_{\text{cmc}} \quad (2)$$

where γ_0 is the surface tension measured for pure water at the appropriate temperature.

Surface excess concentration

The surface excess can be calculated with the Gibbs equation:

$$\Gamma = -10^{-7}(1/RT)(d\gamma/d \ln C)_T \quad (3)$$

where Γ is the surface excess concentration of the surfactant (mol/cm^2), R is the gas constant

($R = 8.314 \text{ J/mol K}$), T is the temperature (K), γ is the surface or interfacial tension (mN/m), and C is the concentration of the surfactant (mol/L).¹⁹

Minimum surface area per molecule

The average area occupied by each adsorbed molecule at the interface is given by

$$A_{\min} = 10^{16}/[\Gamma_{\max} \times N_A] \quad (4)$$

where A_{\min} is the surface area per molecule of solute (nm^2), Γ_{\max} is the surface excess concentration (mol/ m^2), and N_A is Avogadro's number.^{20,21}

Gibbs free energy of micellization (ΔG_{mic})

Information on the free energy of micellization was obtained indirectly from the cmc values with the following equation:²²

$$\Delta G_{\text{mic}} = RT(1 + \alpha) \ln \text{cmc} \quad (5)$$

where T is the absolute temperature and α is the fraction of counterions bound by the micelle in the case of ionic surfactants ($\alpha = 0$ for a nonionic surfactant).²³

Gibbs free energy of adsorption (ΔG_{ads})

ΔG_{ads} was calculated with the following equation:^{24,25}

$$\Delta G_{\text{ads}} = \Delta G_{\text{mic}} - (0.6022 \times \pi_{\text{cmc}} \times A_{\min})$$

Photography and kinetic study of the demulsification process

Three demulsifiers (D4, D1, and BIa) were chosen for this purpose on the basis of their demulsification efficiency (low, moderate, and high, respectively). The 70% W/O emulsion was kept overnight at room temperature to get a stable emulsion without treatment. Photographic microscopy studies were carried out at 60°C for treated and untreated emulsions. The treated and untreated emulsion samples were taken at different times with a Teflon stick for analysis. An emulsion droplet was spread on a glass slide and covered with a Teflon layer. The slides were photographed under an Olympus binocular microscope (Germany) with a camera, and the droplets were counted with the help of a Digitat 5050-R (Germany).²⁶

RESULTS AND DISCUSSION

Chemical structure confirmation

The FTIR spectra of PSMA and typical esterified PSMA samples are shown in Figure 1. The absorp-

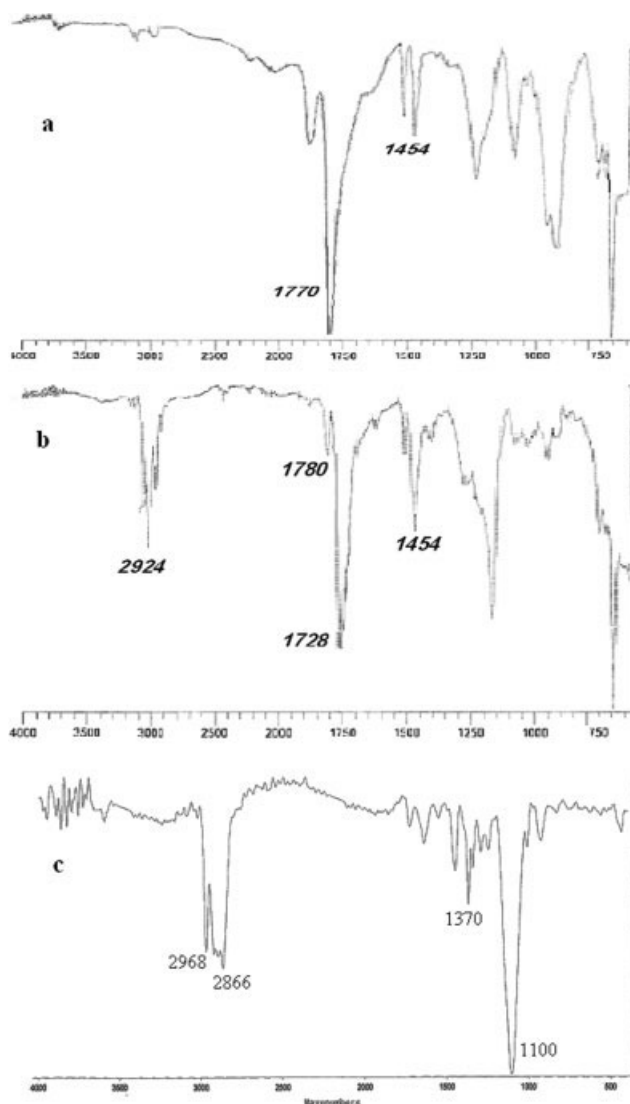


Figure 1 FTIR spectra for (a) PSMA, (b) MPSMA, and (c) DPSMA.

tion peaks centered at 1770 and 1851 cm^{-1} are the characteristic bands of PSMA, which correspond to the absorption of C=O of the anhydride groups in the five-member ring. In the spectrum of PSMA-12C, there are additional strong absorption bands at 2923 and 2854 cm^{-1} assigned to $\nu_{\text{as}}(\text{CH}_2)$ and $\nu_{\text{s}}(\text{CH}_2)$ of the alkyl ester group. The intensity of the absorption bands due to C=O of the anhydride groups decreases after esterification, and the band position is shifted to a lower wave number from 1734 to 1710 cm^{-1} . The figure also shows the appearance of a strong band at 1104 cm^{-1} assigned to C—O ether bonds in PPO and PEO in the block copolymer. Figure 2 shows the $^1\text{H-NMR}$ spectra of the same samples with structural assignments; the PSMA copolymer shows peaks at 2.15 ppm for the hydrogen of the anhydride group, which disappeared after

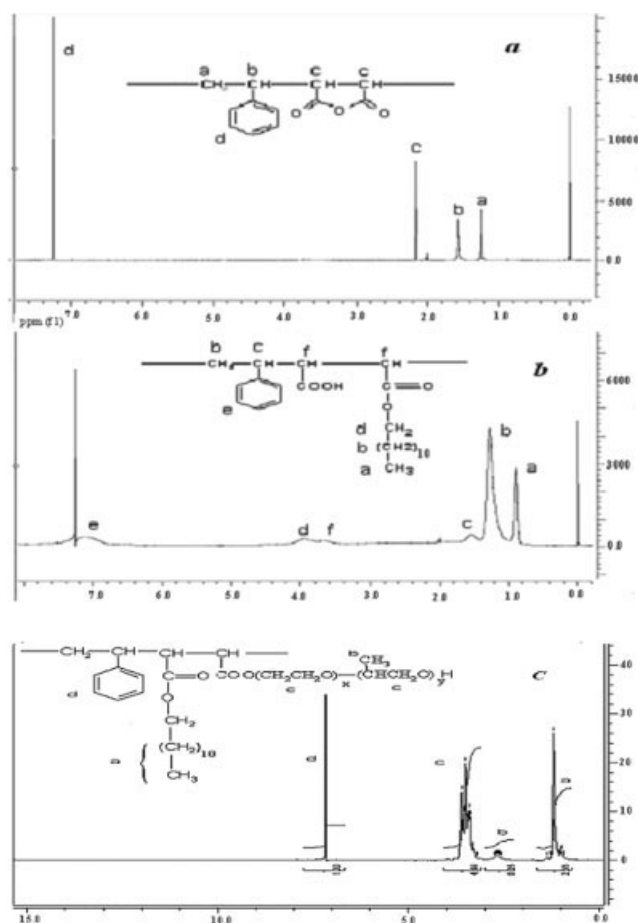


Figure 2 $^1\text{H-NMR}$ spectra for (a) PSMA, (b) MPSMA, and (c) DPSMA.

esterification, and a peak at 0.9 ppm for CH_3 of the ester group appears [Fig. 2(b)] in addition to a weak band at 4.0 ppm for the $-\text{O}-\text{CH}_2$ group and a strong one at 1.3 ppm for $-(\text{CH}_2)_{10}-$. The presence of the block PPO-PEO copolymer is confirmed by the strong peak appearing at 3.2 ppm, which is due to the many $\text{O}-\text{CH}_2$ groups.

Factors affecting the demulsification efficiency

Effect of the chemical structure

Chemical demulsification is an important method of treating W/O emulsions. Amphiphilic block copolymers that contain PPO as a hydrophobic part and PEO as a hydrophilic part in different ratios are commercially available and are widely used.^{6,27} However, our preliminary investigations on our crude oil emulsions indicate that the newly prepared materials in this work are superior to the commercial PPO-PEO block polymers. Our samples contain a hydrophobic backbone in addition to the more hydrophilic side chain; the hydrophobic segments, which are oil-soluble, can then match the asphaltenic fraction of the

TABLE II
Demulsification Efficiency of Treated and Untreated Crude Oil Emulsions (with Water Contents of 30, 50, and 70%) with Different Concentrations of Individual Demulsifiers at 60°C

Demulsifier	Concentration (ppm)	Water content (%)	Time (min)	Demulsifier efficiency (%)
Blank	0	30	65 ^a	30
		50	53 ^a	52
		70	48 ^a	71
D1	50	30	180	63
		50		64
		70		74
D2	100	30	150	73
		50		80
		70		96
D3	50	30	240	55
		50		66
		70		86
D4	100	30	210	70
		50		86
		70		90
D3	50	30	270	50
		50		68
		70		83
D4	100	30	270	73
		50		78
		70		85
D4	50	30	300	47
		50		52
		70		58
D4	100	30	300	53
		50		58

^a Days instead of minutes.

crude oil, thus enhancing the demulsification efficiency. The demulsification efficiency data for the four individual demulsifiers with different molecular weights and PPO/PEO ratios prepared in this work are shown in Table II, whereas Figures 3 and 4 illustrate the kinetics of water separation. By the inspec-

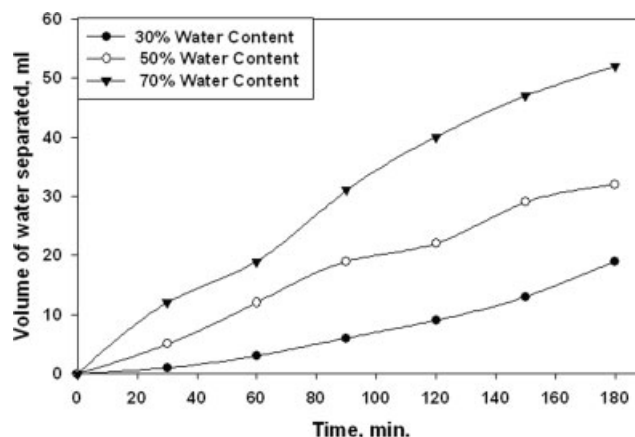


Figure 3 Demulsification process of D1 at 50 ppm and 60°C.

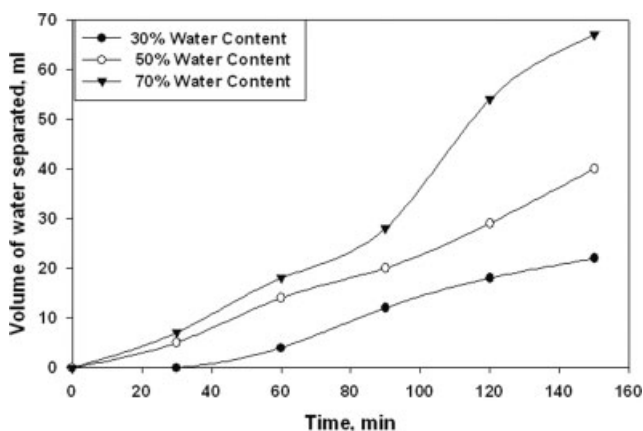


Figure 4 Demulsification process of D1 at 100 ppm and 60°C.

tion of the obtained data, it was found that the blank crude oil had a very slow rate of demulsification (demulsification efficiency = 71%) after 48 days, whereas the maximum demulsification efficiency was obtained with the individual demulsifier D1. The demulsification efficiency decreased for D2, D3, and D4, and this could be due to several factors:

1. An increase in the molecular weight may lead to lower mobility of the demulsifier in the emulsion. Some investigators^{23,28} have studied the relationship between the molecular weight of demulsifiers and their efficiency and found a direct relation between the molecular weight and efficiency of demulsifiers. The data obtained in this work, as shown in Figure 5, which describe the relationship between the PPO/PEO ratio and molecular weight and the demulsification efficiency, do not agree with their findings.
2. The demulsification efficiency is very sensitive to the PPO/PEO ratio. It increases as this ratio increases up to unity, at which the oil resolution is the highest.²⁹ A decrease in the PPO/PEO ratio leads to an increase in the hydrophilic part in the demulsifier molecule, which increases the affinity of the molecule to the coil. This coiling may hinder the adsorption of the demulsifier molecules on the oil/water interface, and so the demulsification efficiency decreases. This means that the coalescence of water droplets become more difficult.³⁰

Effect of the demulsifier concentration

One of the most important parameters governing the adsorption of demulsifiers at the interface is the demulsifier concentration.²³ The effects of four demulsifiers (D1, D2, D3, and D4) on the dewatering percent-

age are shown in Table II. The water separation accelerates with an increase in the demulsifier concentration. These data indicate that increasing the demulsifier concentration leads to an increase in the adsorption of the demulsifier molecules on the W/O interface, which thus replace the native emulsifiers (asphaltene); this causes the mechanical stability of the interfacial film. The stability of this film continues to decrease, and it gets thinner until it collapses totally with further adsorption of the demulsifier agent.¹⁸

Effect of the water content

From the data in Table II and the illustrations in Figures 4 and 5, it is clear that the demulsification efficiency increases with increasing water content from 30 to 70% for all the investigated demulsifiers. This may be attributed to the water content in the W/O emulsion because the repulsion of the W/O interface depends on the pressure of both the internal (water) and external (oil) phases, so at a low water content, the internal pressure of a water droplet is lower than the external pressure of an oil droplet.¹⁶ This leads to an increase in the mechanical stability of the W/O interface and rigidity of the film. On the other hand, the rigidity of W/O films decreases with increasing water content in the bulk until the internal pressure becomes greater than the external pressure. At that moment, a rapid rupture of the W/O interface occurs, and the coalescence of water droplets increases.

Effect of the demulsifier blend

Usually, commercial demulsifiers are blend mixtures of more than one component that have various

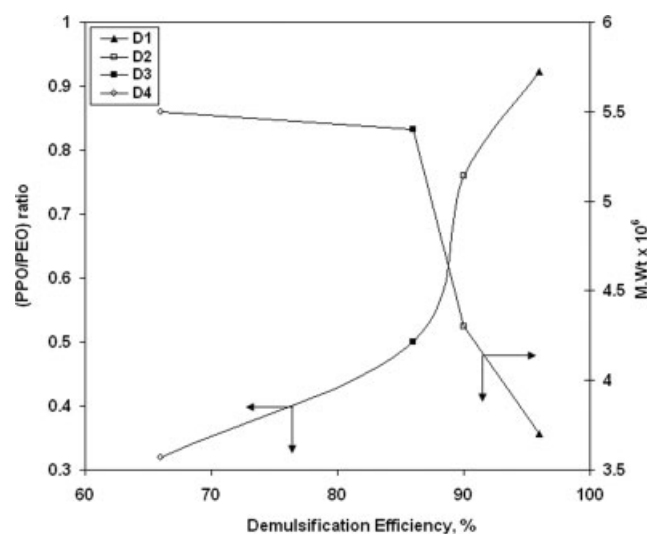


Figure 5 Effect of the molecular weight and PPO/PEO ratio on the demulsification efficiency of the individual demulsifiers.

TABLE III
Demulsifier Blend Ingredients and Their Demulsification Efficiency at 100 ppm and 60°C with a Water Concentration of 70%

Demulsifier blend	Individual demulsifier ratio	Code	Time (min)	Demulsification efficiency (%)
D1 : D2	3 : 1	BIa	75	100
	1 : 1	Bib	90	100
	1 : 3	B1c	120	100
D1 : D3	3 : 1	BIIa	90	100
	1 : 1	BIIIb	105	100
	1 : 3	BIIc	120	100
D1 : D4	3 : 1	BIIIa	210	94.3
	1 : 1	BIIIB	210	90
	1 : 3	BIIIC	270	84.3
D2 : D4	3 : 1	BIVa	270	100
	1 : 1	BIVb	270	100
	1 : 3	BIVc	270	100

chemical structures; also, polymeric materials with wide molecular weight distributions can be used for this purpose. In this work, polymeric blend demulsifiers possessing different PPO/PEO ratios were used. The blends were based basically on the demulsifier D1, which exhibited the maximum efficiency individually, and the D2, D3, and D4 demulsifiers were added to it in three different ratios: 3 : 1, 1 : 1, and 1 : 3, respectively. The demulsifier blend ingredients and their demulsification efficiency are depicted in Table III. Figure 6 presents the kinetics of water separation with demulsifier blends, which exhibited the maximum efficiency of demulsification at the minimum time taken for complete water separation. It was found that, in general, the blends exhibited greater efficiency than that obtained by the individual demulsifiers, as shown in Table II. The data show that the blends had a positive synergetic effect that increased with an increasing D1 ratio. BI exhibited the maximum demulsification efficiency, and the lowest efficiency was obtained by BIV. The ratio of the individual mixtures plays an important role in the efficiency of the blend. From the data in Table III, it was confirmed that the most effective ratio is 3 : 1 D1 to D2, D3, or D4. At this mixed ratio, the lowest times taken for complete water separation were 75, 90, 210, and 270 min for BIa, BIIa, BIIIa, and BIVa, respectively.

Surface tension parameters

The data for the surface-active parameters and demulsification efficiency (%) of the prepared demulsifiers are tabulated in Table IV. It is obvious that the cmc values decrease with the temperature increasing from 25 to 45°C for all tested demulsifiers. This is because increasing the temperature leads to

an increase in the mobility of the demulsifier (as shown in Fig. 7), which might be adsorbed onto the W/O interface. Table IV and Figure 8 show that cmc (mol/cm^3) decreases with an increasing PPO/PEO ratio as well as the demulsification efficiency. The increase in the PPO/PEO ratios leads to increased adsorption of the demulsifier molecules on the W/O interface as a result of the increasingly hydrophobic character of the demulsifier.

The values of Γ_{max} and A_{min} are listed in Table IV. It is evident that A_{min} increases with increasing temperature; this is probably due to the increase in thermal motion.^{31,32} However, A_{min} decreases with a decreasing PPO/PEO ratio of the demulsifiers. This may be attributed to the increase in the hydrophilic ethylene oxide units in the copolymer, which leads to an increase in the surface area occupied by the surfactant (demulsifier) molecules. A similar conclusion was reported by other authors.^{31,33} The results for the thermodynamic parameters of micellization, expressed by ΔG_{mic} and ΔG_{ads} , of the demulsifiers are listed in Table IV. Because ΔG_{mic} is less than 0, micellization is a spontaneous process; in addition, ΔG_{mic} becomes less negative with an increase in the ethylene oxide units, which leads to the steric inhibition of micellization.³² The ΔG_{ads} negative values are greater than ΔG_{mic} , indicating that the demulsifiers prefer to adsorb on the interface than to form micelles. Because the adsorption on the interface is associated with a decrease in the free energy of the system, there is a direct relationship between the efficiency of the demulsifiers and the values of ΔG_{ads} . In this respect, the maximum $-\Delta G_{\text{ads}}$ (-41.80 kJ/mol) was obtained with D1, which exhibited the highest demulsification efficiency (96%), and the minimum $-\Delta G_{\text{ads}}$ (-36.08 kJ/mol) was obtained with D4, which had the lowest demulsification efficiency (66%).

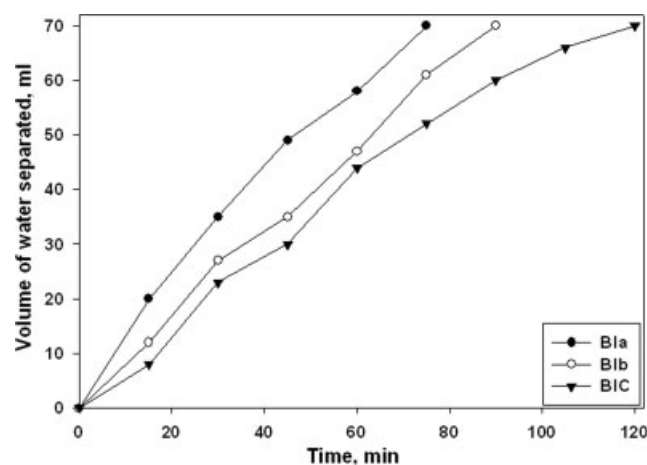


Figure 6 Demulsification process of the BI group at 100 ppm and 60°C with a water concentration of 70%.

TABLE IV
Surface-Active and Thermodynamic Properties and PPO/PEO Ratios of Individual Demulsifiers
at Different Temperatures

Demulsifier	Temperature (°C)	cmc (mol/L)	γ_{cmc} (mN/m)	Γ_{max} ($\times 10^{10}$ mol/m ²)	A_{min} (nm ²)	π_{cmc} (mN/m)	ΔG_{mic} (kJ/mol)	ΔG_{ads} (kJ/mol)	PPO/PEO ratio
D1	25	7.69×10^{-8}	30.0	3.42	48.58	42	-40.58	-41.81	0.92
	35	6.45×10^{-8}	29.0	3.17	52.31	41	-42.40	-43.69	
	45	4.23×10^{-8}	28.0	2.68	61.86	40	-44.89	-46.38	
D2	25	8.33×10^{-8}	31.0	3.10	53.55	41	-40.39	-41.71	0.76
	35	7.28×10^{-8}	29.0	2.69	61.72	41	-42.09	-43.61	
	45	5.63×10^{-8}	28.5	2.33	71.26	39.5	-44.13	-45.83	
D3	25	9.15×10^{-8}	32.0	2.96	55.00	40	-40.15	-41.47	0.5
	35	5.75×10^{-8}	30.0	2.86	58.09	40	-42.69	-44.09	
	45	6.55×10^{-8}	29.5	2.65	62.65	38.5	-43.73	-45.18	
D4	25	8.15×10^{-7}	33.0	2.71	56.98	39	-34.74	-36.08	0.32
	35	5.75×10^{-7}	31.0	2.54	62.89	39	-36.79	-38.27	
	45	3.88×10^{-7}	29.5	2.35	70.65	38.5	-39.03	-40.67	

Photography and kinetics of the demulsification process

W/O emulsion photographs for the control and B1a samples as representative examples are shown in Plate 1 as a function of time. From the photographs, one can see that the size of the water droplet increases with time. Table V lists the coalescence parameters of the 70% W/O emulsion and also the control sample at 60°C.

The increased water droplet radius leads to an increase in the coalescence rate. These data can be analyzed through the plotting of the specific surface area of the water droplet against time, as shown in Figures 9–12. These plots can be conveniently split into two or three segments, and each line of the straight segments is described by a first-order rate equation as follows:

$$\log s = -kt + c \quad (6)$$

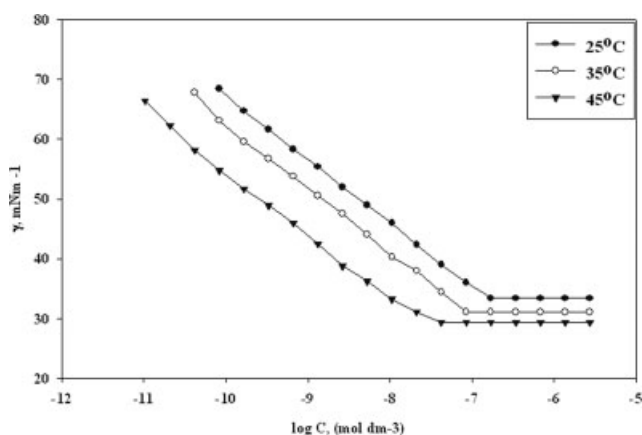


Figure 7 Surface tension (γ) versus the logarithm of the solute concentration ($\log C$) of D1 at different temperatures.

where s is the interfacial area per gram of dispersed phase. c is a constant and k is the slope of each line and is measured by the coalescence rate during that period:

$$k = \frac{d \log s}{dt} \quad (7)$$

By analyzing the data in Table V and the illustrations in Figures 9–12, we have found that the demulsification process can be divided into two or three main steps depending on the demulsification power of the used demulsifier: (A) adsorption and flocculation, in which the demulsifiers adsorb and displace the natural surfactant existing on the W/O interface; (B) coalescence, in which two neighbor water droplets approach each other to form microclusters with

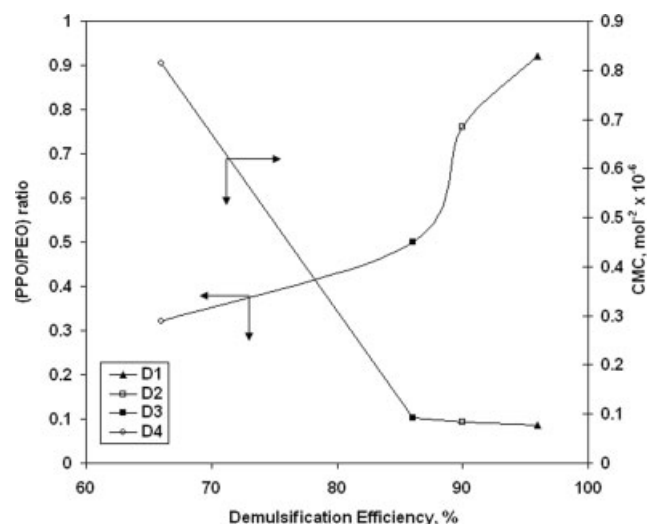


Figure 8 Relation between the cmc value and PPO/PEO ratio and the demulsification efficiency of individual demulsifiers.

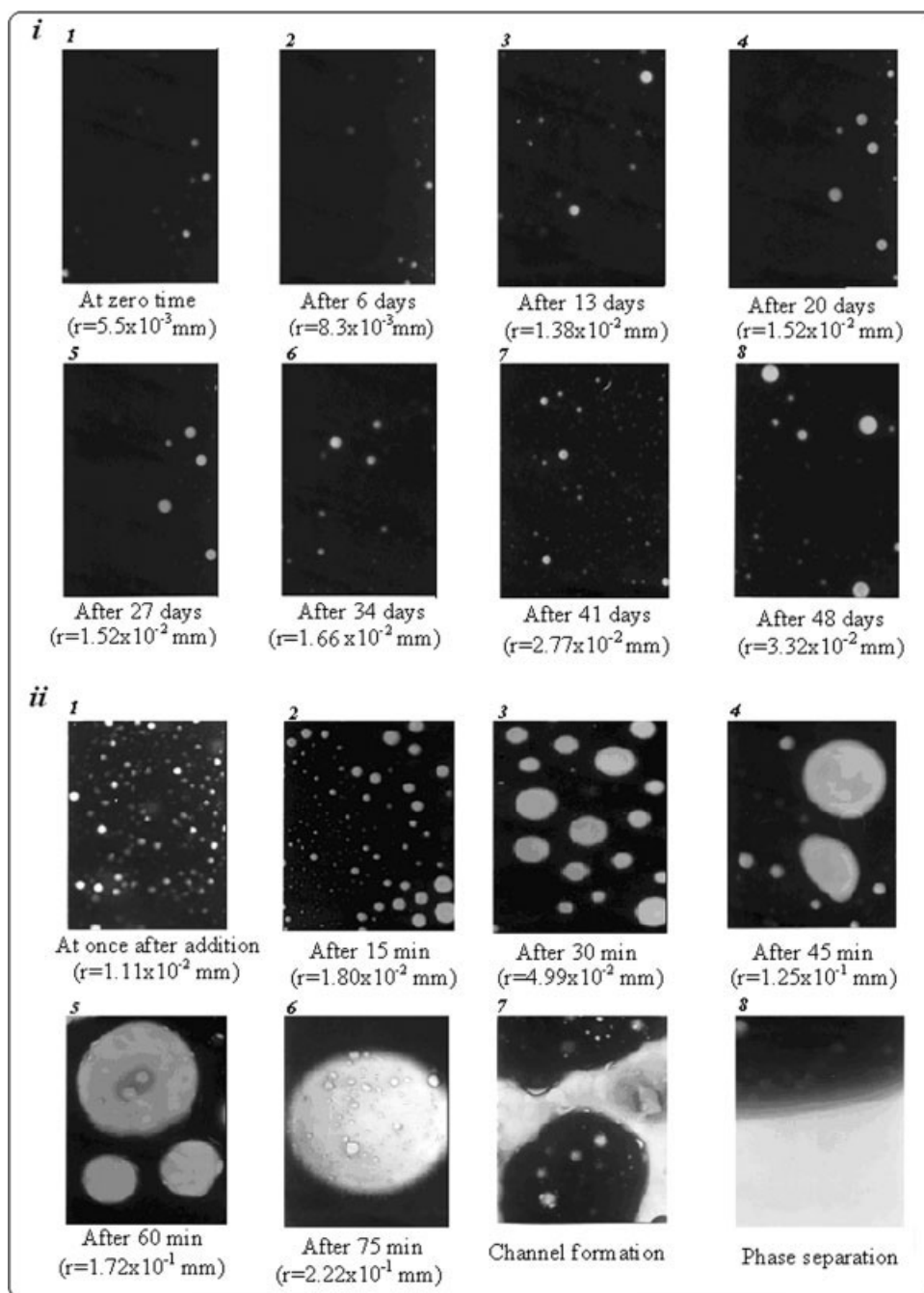


Plate 1 Photographs of (i) a W/O untreated emulsion and (ii) an emulsion treated with the B1a blend demulsifier as a function of time.

low interfacial tension on their W/O interface; and (C) channel formation followed by separation, in which the formed microclusters are collected to form macroclusters and then coagulate to form channels followed by complete water separation.

By following the increasing water droplet diameter in Plate 1, we find that the water droplet size depends on the time of coalescence and the type of demulsifier added. The control sample shows a very

slow increase in the water droplet diameter with time: the diameter of the water droplet increases from 0.0055 to 0.0138 mm after 20 days (step A) and then increases slowly to 0.0277 mm after 34 days (step B), at which a water content of 27% is separated. After 48 days, a water content of only 71% is separated. In the case of the B1a demulsifier, as shown in Figure 12, steps B and C are fused together to give only one step. From this observation, it is

TABLE V
Coalescence Parameters of 70% W/O Treated Emulsions and Untreated Emulsions at 60°C

Demulsifier	Time (min)	r (mm)	Log s	Rate of coalescence
Control	0*	5.54×10^{-3}	2.734	2×10^{-5}
	6*	8.31×10^{-3}	2.558	
	13*	1.39×10^{-2}	2.336	
	20*	1.52×10^{-2}	2.294	2×10^{-6}
	27*	1.52×10^{-2}	2.294	
	34*	1.66×10^{-2}	2.256	
	41*	2.77×10^{-2}	2.035	1×10^{-5}
	48*	3.32×10^{-2}	1.955	
D4	0	1.39×10^{-2}	2.336	5×10^{-3}
	30	1.52×10^{-2}	2.294	
	60	1.66×10^{-2}	2.256	5×10^{-4}
	90	1.80×10^{-2}	2.222	
	120	3.05×10^{-2}	1.993	
	150	5.26×10^{-2}	1.756	1.09×10^{-3}
	180	1.25×10^{-1}	1.381	
	D1	0	1.39×10^{-2}	2.336
30	3.05×10^{-2}	1.993		
60	4.99×10^{-2}	1.779		
90	7.89×10^{-2}	1.580	7.7×10^{-3}	
120	1.75×10^{-1}	1.235		
150	1.94×10^{-1}	1.190	4.2×10^{-3}	
B1a	0	1.11×10^{-2}	2.433	2.37×10^{-2}
	15	1.80×10^{-2}	2.222	
	30	4.99×10^{-2}	1.780	
	45	1.25×10^{-1}	1.381	
	60	1.72×10^{-1}	1.242	8.3×10^{-3}
	75	2.22×10^{-1}	1.132	

* Time taken/day.

evident that the B1a demulsifier exhibits the greatest demulsification performance of the D1 and D4 demulsifiers.

From the data in Table V, the rate of coalescence for the control sample was found to be 2×10^{-5} , 2×10^{-6} , and 1×10^{-5} for steps A, B, and C, respectively. The rate of coalescence of D4 (low

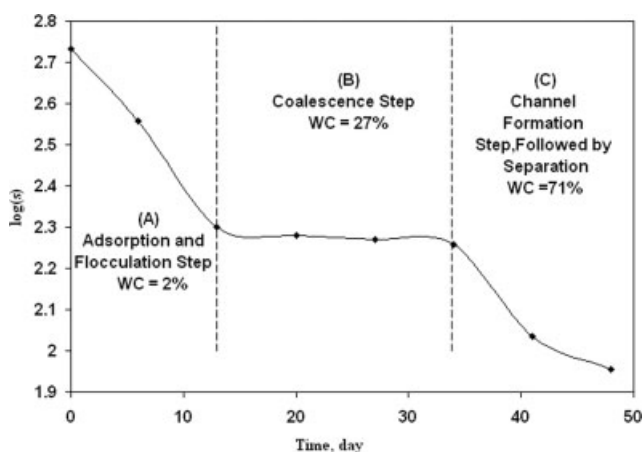


Figure 9 Time taken for the demulsification process against log s for a control sample with a 70% W/O emulsion at 60°C (WC = water content).

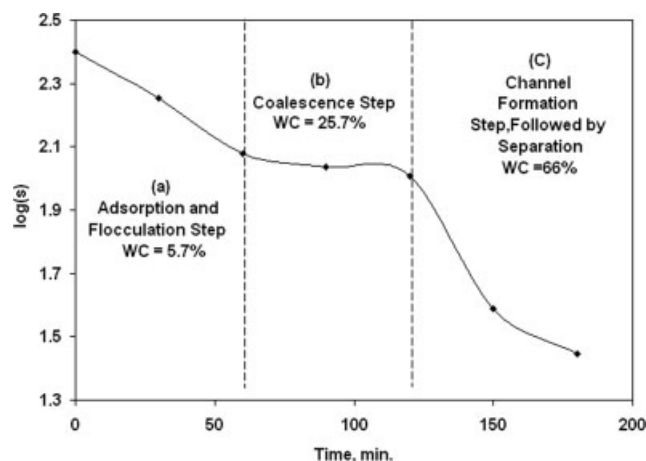


Figure 10 Time taken for the demulsification process against log s for D4 with a 70% W/O emulsion at 100 ppm and 60°C.

demulsification efficiency of 66%) was 5.1×10^{-3} , 1.8×10^{-3} , and 4.8×10^{-3} for the three previous steps (A, B, and C), respectively. However, in the case of B1a (high demulsification efficiency of 100%), the rate of coalescence of step A was very fast and unnoticeable, so the two steps (A and B) merged together to give only one step with a rate of coalescence of 2.37×10^{-2} .

CONCLUSIONS

A styrene/maleic anhydride alternating copolymer was treated with dodecanol [$\text{CH}_3(\text{CH}_2)_{11}\text{—OH}$] to produce a copolymer with long hydrophobic side chains and free carboxylic groups. These carboxylic groups were further esterified with PPO-PEO block copolymers (different PPO-PEO ratios and molecular weights) to produce four different surfactants. These surfactants were investigated as demulsifiers for

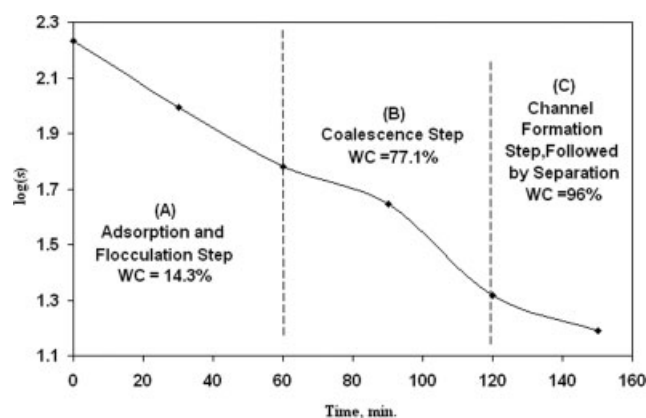


Figure 11 Time taken for the demulsification process against log s for D1 with a 70% W/O emulsion at 100 ppm and 60°C.

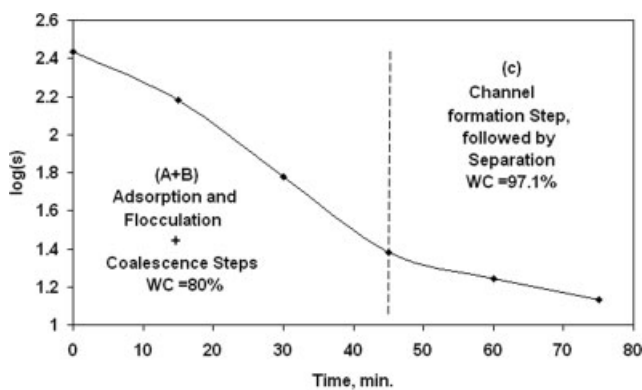


Figure 12 Time taken for the demulsification process against $\log s$ for the B1a blend with a 70% W/O emulsion at 100 ppm and 60°C.

W/O emulsions. The maximum demulsification efficiency was obtained by the demulsifier D1 (which has the lowest molecular weight and the highest PPO–PEO ratio). It seems that the presence of the phenyl group in PSMA matches the asphaltenic fractions of the crude oil, and this may explain the higher demulsifying efficiency of the prepared demulsifiers over the commercial block copolymers.

Blending of the individual demulsifiers was performed through the blending of the most efficient individual demulsifier, D1, with the other demulsifiers in different ratios, and it was found that the blends had a synergetic effect. The maximum synergism was obtained through the blending of D1 and D2 in a 3 : 1 ratio to produce the mixed surfactant labeled B1a.

The surface-active and thermodynamic properties for the individual demulsifiers showed that ΔG_{ads} was greater than ΔG_{mic} for all of them, and the obtained results showed a strong relation between these parameters and the demulsification efficiency.

The kinetic properties of the demulsification process were investigated for an untreated emulsion and emulsions treated with D4, D1, and B1a. The demulsification mechanism was found to occur in three stages: adsorption and flocculation, coalescence, and channel formation followed by separation. For the untreated emulsion, the rate of coalescence was very slow (the rate of coalescence of the control sample was 2×10^{-5} , 2×10^{-6} , and 1×10^{-5} for steps A, B, and C, respectively). The rate of the treated emulsions was accelerated from D4, the least effective demulsifier, to D1, the most effective individual demulsifier, whereas with the emulsion treated with B1a, the most effective blend, the rate of coalescence increased to very high values, so that

steps A and B of the coalescence merged into one step, and the rates of coalescence were 2.37×10^{-2} and 8.31×10^{-5} for steps A–B and C, respectively.

References

- Djuve, J.; Yang, X.; Fjellanger, I. *Colloid Polym Sci* 2001, 279, 232.
- Joseph, D. M.; Peter, K. K. *J Colloid Interface Sci* 1997, 189, 242.
- Wu, J.; Xu, Y.; Dabros, T.; Hamza, H. *Colloids Surf A* 2005, 252, 79.
- Bhardwaj, A.; Hartland, S. *Ind Eng Chem Res* 1994, 33, 1271.
- Zhiqing, Z.; Xu, G. Y.; Wang, F.; Dong, S. L.; Li, Y. M. *J Colloid Interface Sci* 2004, 277, 464.
- Mohammed, R. A.; Baily, A. I.; Lickham, P. F.; Taylor, S. E. *Colloids Surf A* 1993, 80, 237.
- Mohammed, R. A.; Baily, A. I.; Lickham, P. F.; Taylor, S. E. *Colloids Surf A* 1994, 83, 261.
- Zapryanov, Z.; Malhotra, A. K.; Aderangi, N.; Wasan, D. T. *Int J Multiphase Flow* 1983, 9, 105.
- Djuve, J.; Yang, X.; Fjellanger, I. J.; Sjoblom, J.; Pelizzetti, E. *Colloid Polym Sci* 2001, 279, 232.
- Kanga, W.; Jing, G.; Zhang, H.; Li, M.; Wu, Z. *Colloids Surf A* 2006, 272, 27.
- Kim, Y. H.; Wasan, D. T. *Ind Eng Chem Res* 1996, 35, 1141.
- Shetty, C. S.; Nikolov, A. D.; Wasan, D. T. *J Dispersion Sci Technol* 1992, 13, 121.
- Marquez-Silva, R. L.; Key, S.; Marino, J.; Guzman, C.; Buitrago, S. *SPE* 1997, 37, 271.
- Li, C.; Pan, X.; Hua, C.; Su, J.; Tian, H. *Eur Polym J* 2003, 39, 1091.
- Kim, Y. H.; Wasan, D. T. *Ind Eng Chem Res* 1996, 35, 1141.
- Zaki, N. N.; Al-Sabagh, A. M. *Tens Surf Deter* 1997, 34, 12.
- Rosen, M. J.; Aronson, S. *Colloids Surf* 1981, 3, 201.
- Al-Sabagh, A. M.; Abdul-Raouf, M. E.; Abdel-Raheem, R. *Colloids Surf A* 2004, 251, 167.
- Al-Sabagh, A. M. *Polym Adv Technol* 2000, 11, 48.
- Rosen, M. J. *Surfactants and Interfacial Phenomena*; Wiley: New York, 1978.
- Wu, C.; Zhang, J. L.; Li, W.; Wu, N. *Fuel* 2005, 84, 2093.
- Schramm, L. L. *Surfactants: Fundamentals and Applications in Petroleum Industry*; Cambridge University Press: Cambridge, England, 2000.
- Young, K. H.; Darsh, W. T. *Ind Eng Chem Res* 1996, 35, 1141.
- Rosen, M. J.; Aronson, S. *Colloids Surf* 1981, 3, 201.
- Gibbs, J. W. *The Collected Works of J. W. Gibbs*; Longman: London, 1928; Vol. 1, p 119.
- Bharadwaj, A.; Hartland, S. *Ind Eng Chem Res* 1994, 33, 1271.
- Guo, C.; Wang, J.; Liu, H.-Z.; Chen, J.-Y. *Langmuir* 1999, 15, 2703.
- Cooper, D. G.; Zajig, J. E.; Cannel, E. J.; Word, J. W. *Can J Chem Eng* 1980, 58, 576.
- Xu, Y.; Wu, J.; Dabros, T.; Hanza, H. *Energy Fuels* 2005, 19, 3.
- Kang, W. L.; Jing, G. Z.; Zhang, H.; Li, M.; Wu, Z. *Colloids Surf A* 2006, 272, 27.
- Rosen, M.; Dahanayake, M.; Cohen, A. *Colloids Surf* 1983, 5, 159.
- Dahanayake, M.; Cohen, S. W.; Rosen, M. *J Phys Chem* 1986, 90, 2413.
- Al-Sabagh, A. M.; Kandil, N. G.; Badawi, A. M.; El-Sharkawy, H. *Colloid Surf A* 2000, 170, 127.